



# Velocity and concentration distributions in globally unstable axisymmetric helium jets

Sami Boujema<sup>a,b</sup>, Muriel Amielh<sup>a,\*</sup>, Marie Pierre Chauve<sup>a</sup>

<sup>a</sup> *Institut de recherche sur les phénomènes hors équilibre, technopôle Château Gombert, 49, rue F. Joliot-Curie, B.P. 146, 13384 Marseille cedex 13, France*

<sup>b</sup> *Faculté des sciences de Tunis, département de physique, campus universitaire Le Belvédère, 1060 Tunis, Tunisia*

Received 14 March 2007; accepted after revision 22 May 2007

Available online 3 July 2007

Presented by Paul Clavin

---

## Abstract

We study the distribution of the velocities and concentrations in the near-field of axisymmetric pure helium jets, issuing into air at rest. Helium mass concentrations are deduced from O<sub>2</sub> partial pressure measurements and velocity profiles are obtained by laser Doppler velocimetry. The characteristic frequencies of the globally unstable jets are deduced from fast flow visualization and associated image processing. *To cite this article: S. Boujema et al., C. R. Mecanique 335 (2007).*

© 2007 Académie des sciences. Published by Elsevier Masson SAS. All rights reserved.

## Résumé

**Distributions de vitesses et de concentrations dans des jets axisymétriques d'hélium globalement instables.** Nous étudions la distribution des vitesses et des concentrations dans des jets axisymétriques d'hélium pur en proche sortie de buse, s'épanouissant dans de l'air au repos. Les concentrations massiques d'hélium sont obtenues via des mesures de pression partielle d'oxygène et les vitesses sont obtenues par vélocimétrie laser Doppler. Les fréquences caractéristiques des jets globalement instables sont déduites de l'analyse d'images obtenues par visualisation rapide. *Pour citer cet article : S. Boujema et al., C. R. Mecanique 335 (2007).*

© 2007 Académie des sciences. Published by Elsevier Masson SAS. All rights reserved.

*Keywords:* Fluid mechanics; Jet; Instability; Variable density

*Mots-clés:* Mécanique des fluides ; Jet ; Instabilité ; Masse volumique variable

---

## 1. Introduction

In the literature, many works have been devoted to the studies of the instabilities which develop in low-density axisymmetric jets, with or without gravity effect. These previous experimental or theoretical papers were generally focused on the study of the thresholds of instabilities and on the characteristic frequencies of the flow [1–3] but, only a few studies aimed at obtaining the distribution of the average mass-concentration in order to compare it with the

---

\* Corresponding author.

*E-mail address:* [muriel.amielh@irphe.univ-mrs.fr](mailto:muriel.amielh@irphe.univ-mrs.fr) (M. Amielh).

velocity distribution, especially for low Reynolds numbers, in areas close to the nozzle exit [4]. Furthermore, the linear theories use assumptions, as the quasi-parallel flow one, which imply, amongst other things, a specific behavior of the average scalar (concentration) field. Thus, it appeared useful, as it is suggested in a very recent paper [5], to present experimental results which mainly concern concentrations, velocities and frequencies measurements, obtained in a pure helium jet issuing into ambient air at rest, as it can be seen on the instantaneous visualization (Fig. 1) of a  $12D$  field at Reynolds number  $Re = U_j D / \nu = 576$  (where  $U_j$  is the exit velocity and  $\nu$  the helium kinematic viscosity).

## 2. Experimental setup

The experimental device has been well described in previous articles [6,7]. We just recall that the helium flow is carried by a vertical axisymmetric tube to a convergent nozzle with an exit diameter  $D = 15$  mm and a contraction ratio of 6. The jet issues into a square channel ( $300 \times 300 \times 800$  mm<sup>3</sup>) and evolves in the ambient air at rest. The velocity measurements are performed with a laser Doppler velocimeter (Flowlite DANTEC) with a  $0.8 \times 0.09 \times 0.09$  mm<sup>3</sup> probe volume. For these measurements and also for the jet visualizations by fast video, the flow was seeded by micrometric oil particles, generated by aroma diffusers placed in the input circuit. The radial profiles of the streamwise velocity component are established in the privileged direction, orthogonal to the laser beam plane, in order to limit the errors of space integration of the measurement, mostly in the region of strong gradients corresponding to the jet edge. The mass concentration values in the helium/air mixtures are carried out by using a zirconium electrochemical micro-gauge (SETNAG, ATK10 type) connected to an aspirating probe of 1 mm diameter. This apparatus measures the quantity of oxygen contained in a gas mixture and gives an electric tension proportional to the volume fraction of oxygen. Then, the values of the mass fraction  $C$  and the density  $\rho$  values are obtained by using the relation between the two parameters which is  $1/\rho = C/\rho_{\text{He}} + (1 - C)/\rho_{\text{Air}}$ . In addition, it was checked that the presence of the aspiration probe in the flow modified neither the jet frequency, nor the mean velocity profiles. Axial measurements of the mass concentration and also radial measurements in the sections located at  $2D$  and  $6D$  from the nozzle exit are performed, for two characteristic values of the Reynolds number ( $Re = 280$  and  $600$ ). Indeed, it should be specified that beyond  $Z/D = 6$  and for  $Re = 600$ , the jet evolves to a turbulent state with contingent side ejections. Fig. 1 illustrates these side ejections that can be observed (Fig. 1(b)) or not (Fig. 1(a)) for the same initial ejection conditions. For all the other results, the Reynolds numbers presently vary in the range of values from 230 to 1000 which corresponds to a variation of the Richardson number  $Ri = gD(1 - S)/SU_j^2$  in the range 0.02–0.34 (where  $g$  is the gravity acceleration and  $S = \rho_{\text{He}}/\rho_{\text{Air}} = 0.14$  is the initial density ratio).

## 3. Results

The exit radial velocity profiles of ‘top-hat’ type are given in Fig. 2 where the radial coordinate is normalized by the momentum thickness  $\theta$  calculated at the nozzle exit and shown to verify the law  $\theta/D = A Re^{-1/2}$  with  $A = 0.87$  [6]. For the range of Reynolds numbers corresponding to our study and due to the very good similarity of the experimental profiles, the vorticity thickness at the exit  $\theta_\omega$  verifies the law  $\theta_\omega/D = B Re^{-1/2}$  where  $B = 3.3$  (value which varies according to authors). In Fig. 2, it seems that the analytical law  $U/U_j = 0.5 + 0.5 \tanh[(D/8\theta)((L_u/r) - (r/L_u))]$  suggested by Michalke [8] (where  $r$  is the local radius and  $L_u$  the velocity half-width) and often used as an initial profile in numerical and theoretical studies [3,5] does not agree perfectly with our results probably because of the present low Reynolds number values. Otherwise, the exit profile of the mass concentration is obviously a square profile, where  $C = C_j = 1$  on the whole section. This implies that at  $Z/D = 0$ , for any Reynolds number, the profiles of scalar and velocity cannot be similar, contrary to what could occur for a heated jet when a thermal boundary layer develops in the tube, upstream the exit. Figs. 3(a) and (b) give the profiles of the velocity and the concentration, obtained in the two sections and at the Reynolds numbers  $Re = 280$  and  $600$ . Both are normalized by their respective local values  $U_c$  and  $C_c$  on the jet axis and are evaluated versus the local radius normalized respectively by the velocity,  $L_u$ , and concentration,  $L_c$ , half-width. All these values are indicated in Table 1.

Although the Richardson number  $Ri$  is relatively low in this study, buoyancy effects produce a constriction of the jet and an axial acceleration at the exit (Fig. 4). This constriction is confirmed by the half-width values of velocity and concentration  $2L_u/D$  and  $2L_c/D$  which remain lower than 1. At the lowest Reynolds number ( $Re = 280$ ), this effect is clearly stronger on the concentration profile than on the velocity profile and is displayed by a half-width value of concentration equal to the half of the exit nozzle diameter ( $2L_c/D = 0.5$  at  $Z/D = 6$ ). For this same Reynolds

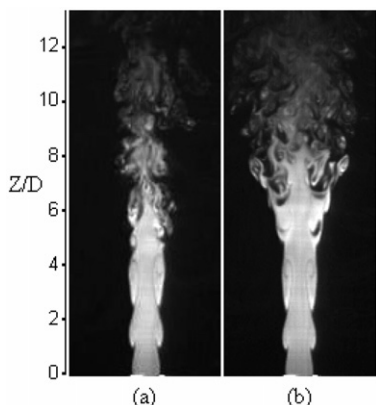


Fig. 1. Helium jet aspect over 12D at  $Re = 576$ , (a) without and (b) with side jets.

Fig. 1. Aspect du jet d'hélium sur 12D à  $Re = 576$ , (a) sans et (b) avec éjections latérales.

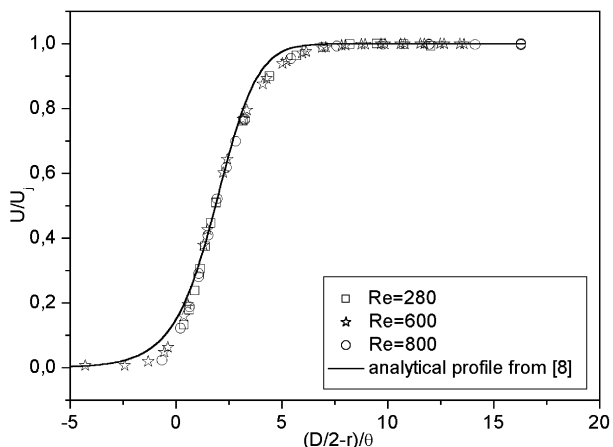


Fig. 2. Comparison of the exit velocity profiles with an analytical profile.

Fig. 2. Comparaison du profil de vitesse en sortie de buse avec un profil analytique.

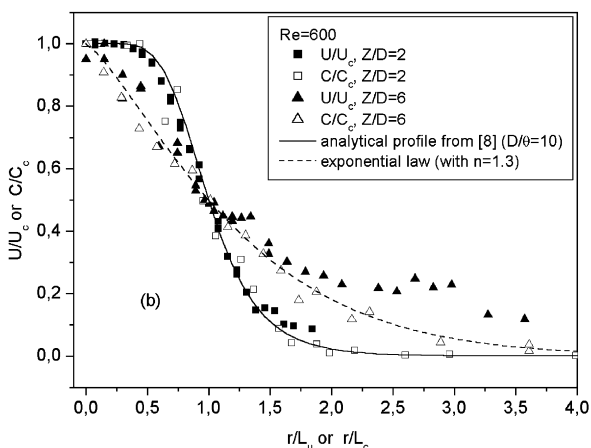
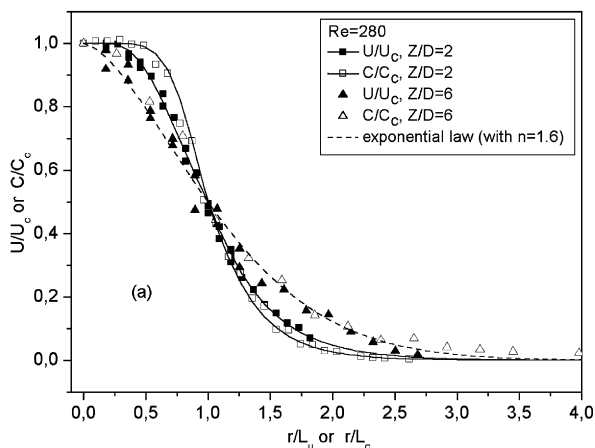


Fig. 3. Radial profiles of velocity and mass concentration at  $Z/D = 2$  and 6, (a) for  $Re = 280$ , (b) for  $Re = 600$ .

Fig. 3. Profils radiaux de vitesse et de concentration massique à  $Z/D = 2$  et 6, (a) for  $Re = 280$ , (b) for  $Re = 600$ .

Table 1  
Experimental conditions  
Tableau 1  
Conditions d'expériences

|         | $U_j$ (m/s) | $Re$ | $Ri$  | $Z/D = 2$       | $Z/D = 6$       |
|---------|-------------|------|-------|-----------------|-----------------|
| Case I  | 2.0         | 280  | 0.23  | $2L_u/D = 0.73$ | $2L_u/D = 0.75$ |
|         |             |      |       | $2L_c/D = 0.69$ | $2L_c/D = 0.50$ |
| Case II | 4.3         | 600  | 0.049 | $2L_u/D = 0.87$ | $2L_u/D = 0.90$ |
|         |             |      |       | $2L_c/D = 0.86$ | $2L_c/D = 0.92$ |

number but at  $Z/D = 2$ , the concentration profile preserves, for longer, a ‘top-hat’ aspect. At  $Z/D = 6$ , this difference in aspect disappears and we can find the same analytical form for both profiles correctly represented by an exponential law  $\exp[-\ln 2(r/L)^n]$ , with  $n = 1.6$  and  $L = L_u$  or  $L_c$ , close to a law of similarity obtained in turbulent jets. For the highest Reynolds number ( $Re = 600$ , Fig. 3(b)), the velocity-concentration similarity is almost respected everywhere

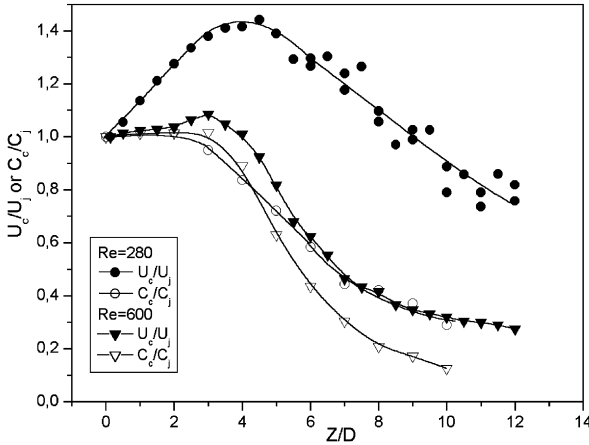


Fig. 4. Streamwise evolutions of velocity and concentration.  
 Fig. 4. Evolutions axiales de vitesse et de concentration.

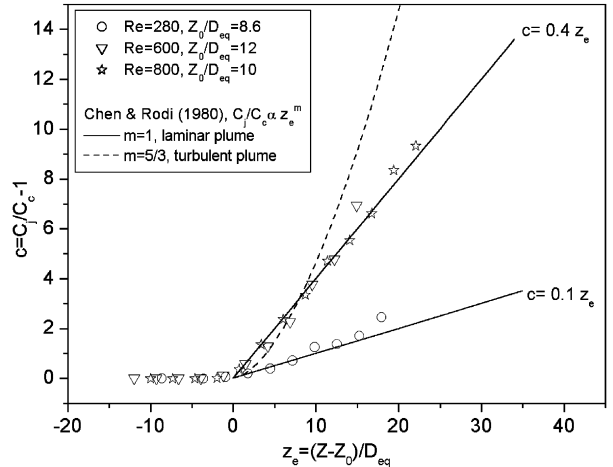


Fig. 5. Axial decay law of the jet concentration.  
 Fig. 5. Lois de décroissance de la concentration sur l'axe du jet.

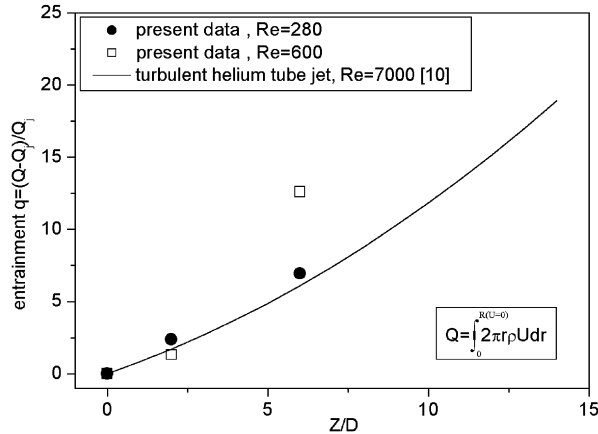


Fig. 6. Evolution of the jet entrainment rate.  
 Fig. 6. Evolution du taux d'entraînement du jet.

except for  $Z/D = 6$  and  $r/L_u$  or  $r/L_c > 2$  where the existence of the strong and random side ejections (Fig. 1(b)) modify significantly the local velocity. At  $Z/D = 2$ , the velocity and concentration evolutions are well represented by the hyperbolic tangent law suggested by Michalke [8] (with  $D/\theta = 10$ ), whereas, at  $Z/D = 6$ , a better agreement is obtained with an exponential law ( $\exp[-\ln 2(r/L)^n]$  with  $n = 1.3$ ). Because of the buoyancy effects at  $Re = 280$ , the axial velocity evolution differs notably from concentration evolution (Fig. 4). The flow is accelerated until  $Z/D = 4$  where the velocity reaches the value of  $1.5U_j$  and then recovers its exit value only at  $Z/D = 10$ . On the other hand, for the two Reynolds numbers  $Re = 280$  or  $600$ , the mixing layer starts to reach the jet axis from the position  $Z/D = 3$  leading to a strong decrease of the axial concentration (Fig. 4). Fig. 5 shows an axial hyperbolic decay ( $m = 1$ ) of the concentration when taking into account a virtual origin  $Z_0$  and the effective diameter  $D_{eq} = DS^{1/2}$  often used in variable density jet works. Although this hyperbolic evolution was already evoked in the review of Chen and Rodi [9] for laminar round plumes, the strong increase of the decay slope between  $Re = 280$  and  $600-800$  (a ratio of 4) is however unusual and is related to the events of side jets which stimulate an efficient mixing when  $Re$  increases. The velocity and concentration profiles are used to evaluate the jet entrainment rate  $q = (Q - Q_j)/Q_j$  (where  $Q$  is the mass rate at the section  $Z/D$  and  $Q_j$  the mass rate at the jet exit) given in Fig. 6 and compared to an entrainment rate obtained in the near-field of a turbulent helium jet [10]. It seems clear that the strong entrainment rate at  $Z/D = 6$  for

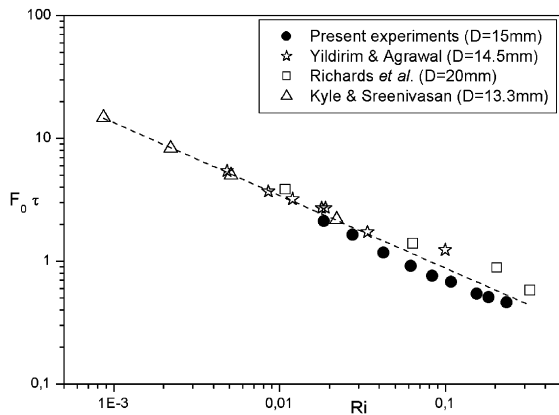


Fig. 7. Fundamental frequency evolution vs. Richardson number, comparison with [1,4,12] data.

Fig. 7. Evolution des fréquences fondamentales en fonction du nombre de Richardson, comparaison avec les données de [1,4,12].

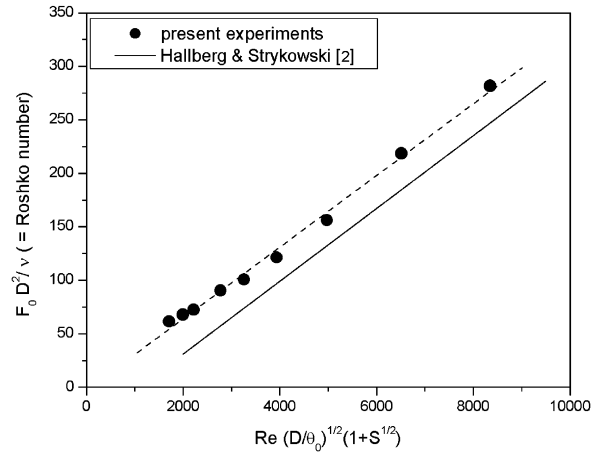


Fig. 8. Roshko number evolution compared with the universal scaling proposed by Hallberg and Strykowski [2].

Fig. 8. Evolution du nombre de Roshko comparée à la loi de Hallberg et Strykowski [2].

$Re = 600$  is in agreement with the efficiency of the mixture quantified by the strong axial decay of the concentration, associated to the side ejections as mentioned by Pasumarthi and Agrawal [11].

In the studied range [230, 1000] of the Reynolds numbers, the helium jet develops under a global mode of instability, for which the jet frequency is constant along the jet column [6,7]. The Strouhal number  $St = F_0 D / U_j$  (where  $F_0$  is the fundamental frequency of the jet oscillations calculated from jet visualizations and associated image processings [6,7]) was shown to vary only slightly according to the Reynolds number (between 0.22 and 0.29). Fig. 7 gives the evolution, according to the Richardson number, of this fundamental frequency  $F_0$  normalised by the characteristic time  $\tau = [DS/g(1-S)]^{1/2}$ , usually used in the studies of plumes without source of velocity and recently raised by [1]. This evolution appears in good agreement with the evolution of fundamental frequencies obtained in other studies of unstable helium jets [1,4,12], in spite of the non-negligible buoyancy effects observed at the lowest Reynolds numbers of this study. Fig. 8 presents the evolution of the Roshko number  $F_0 D^2 / \nu = St Re$  according to a representation introduced by Hallberg and Strykowski [2]. These authors gathered the results of many works under a universal law which would describe, with adapted parameters, the variation of the fundamental frequencies in any axisymmetric jet developing a global mode of instability. In this Fig. 8, the apparent weak gap compared to this law could be attributed to the effects of initial conditions dependent on the development of a boundary layer upstream of the nozzle exit and, in particular to the lowest values of  $D/\theta$  of our experiments. However, it is noticeable that our data follow the same slope. Thus, this rather well agrees with the highlighted analogy in the development of global modes in variable density jets.

#### 4. Conclusion

In the present investigation, the evolutions of the average velocities and concentrations in a self-excited helium jet have been obtained for two characteristic Reynolds numbers and are now available for some comparisons with theoretical or numerical works. Some similarities were found for the axial/radial profiles of velocity and concentration, when the buoyancy effects are lowered and when lateral ejections do not occur in the jet. It has also been demonstrated that the weak effects of buoyancy do not affect the distribution of the jet frequency which joins well the universality of global oscillations in low-density axisymmetric jets.

#### Acknowledgements

The authors acknowledge M. Abid for his comments and remarks in the final drafting of this paper.

**References**

- [1] B.S. Yildirim, A.K. Agrawal, Full-field measurements of self-excited oscillations in momentum-dominated helium jets, *Exp. Fluids* 38 (2005) 161–173.
- [2] M.P. Hallberg, P.J. Strykowski, On the universality of global modes in low-density axisymmetric jets, *J. Fluid Mech.* 569 (2006) 493–507.
- [3] L. Lesshafft, P. Huerre, P. Sagaut, M. Terracol, Nonlinear global modes in hot jets, *J. Fluid Mech.* 554 (2006) 393–409.
- [4] C.D. Richards, B.D. Breuel, R.P. Clark, T.R. Troutt, Concentration measurements in a self-excited jet, *Exp. Fluids* 21 (1996) 103–109.
- [5] M.P. Hallberg, V. Srinivasan, P. Gorse, P.J. Strykowski, Suppression of global modes in low-density axisymmetric jets using coflow, *Phys. Fluids* 19 (2007) 014102-1-9.
- [6] S. Boujemaa, M. Amielh, M.P. Chauve, Analyse spatio-temporelle de jets axisymétriques d'air et d'hélium, *C. R. Mecanique* 332 (2004) 933–939.
- [7] S. Boujemaa, M. Amielh, M.P. Chauve, Space–time analysis of self-excited axisymmetric helium jet, *J. Flow Vis. Image Proc.* 13 (2) (2006) 153–173.
- [8] A. Michalke, Survey on jet instability theory, *Prog. Aerosp. Sci* 21 (1984) 159–199.
- [9] C.J. Chen, W. Rodi, *Vertical Turbulent Buoyant Jets—A Review of Experimental Data*, Pergamon Press, 1980.
- [10] T. Djeridane, Contribution à l'étude expérimentale de jets turbulents axisymétriques à densité variable, Thèse de Doctorat, Université d'Aix-Marseille II, 1994.
- [11] K.S. Pasumarthi, A.K. Agrawal, Schlieren measurements and analysis of concentration field in self-excited helium jets, *Phys. Fluids* 15 (12) (2003) 3683–3692.
- [12] D.M. Kyle, K.R. Sreenivasan, The instability and breakdown of a round variable-density jet, *J. Fluid Mech.* 249 (1993) 619–664.